Eng. Sci., 2022, **18**, 113–120

Engineered Science
DOI: https://dx.doi.org/10.30919/es8d659

Conductive Polyvinyl Alcohol/Silver Nanoparticles Hydrogel Sensor with Large Draw Ratio, High Sensitivity and High Stability for Human Behavior Monitoring

Yufeng Wu,[1,#] Enfu Chen,[1,#] Xiaodi Weng,[2,*] Zhaofeng He,[3,*] Geng Chang,[4] Xuchao Pan,[4,*] Junchen Liu,[1] Kun Huang,[1] Kai Huang[1] and Ming Lei[1,*]

Abstract

In recent years, conductive hydrogels have become popular substrates for flexible sensors because of their good mechanical properties, electrical conductivity, and biocompatibility. In this paper, the authors solved the key problem of complex preparation technology of hydrogels and prepared conductive polyvinyl alcohol/silver nanoparticles (PVA/AgNPs) hydrogels sensor with high tensile, high sensitivity, and high stability systems. They were prepared by a simple and efficient method of doping AgNPs into the three-dimensional network of PVA hydrogels. The sensor had a large draw ratio of over 500% and stability could be demonstrated by the consistency of electrical signals in 1000 cycles of stretching. The embedded AgNPs enabled the hydrogels to obtain good sensing performance. The excellent performance of sensors was also reflected by the sensing resolution of 0.5% deformation and the fast response time of 758 ms. The PVA/AgNPs hydrogel sensor was used for common human behaviors, such as finger and wrist bending, swallowing, and nodding, which could transmit signals sensitively and stably. Overall, the excellent performances of the PVA/AgNPs hydrogels made it possible to be used in flexible wearable devices as sensors and help monitor human behavior.

Keywords: Polyvinyl alcohol; Silver nanoparticles; Hydrogels; Stretch; Sensors.
Received: 03 February 2022; Revised: 17 February 2022; Accepted: 21 February 2022.
Article type: Research article.

1. Introduction

Recently, flexible sensors[1-5] have drawn huge attention due to their application in human-motion monitoring,[6-15] human-machine interfacing,[16-18] soft robotics,[19-22], and artificial skin.[23-27] In most cases, flexible sensing materials consist of an elastic substrate[28,29] (*e.g.*, polydimethylsiloxane, polylactic acid, and polyurethane) and a conductive portion[30-32] (*e.g.*, metal or carbon nanomaterials). The working mechanism of the flexible sensors is to convert external stimuli into electrical signals. People can obtain useful information by collecting, processing, and analyzing the frequency, amplitude, and stability of electrical signals.[33,34] Sensors in human behavior monitoring devices are usually fixed on each joint of the human body. The motion of the joint will lead to the stretching, compression, and torsion of the sensor, which will lead to the change of electrical signal and realize the monitoring of human behavior.[35] However, the flexible sensors made of those substrates have a strong rigidity, and they are not skin free, these sensors cannot sense the stretching of the skin very well. Even though these sensors are flexible and sensitive, they are still difficult to use to monitor the skin behavior of subjects' motors.[36] Therefore, finding soft and skin-free substrates is the key to constructing flexible sensors for human motion detection.

Hydrogels are considered an ideal material[37-39] because of their cross-linked three-dimensional (3D) network structure, which makes them stretchable and compressible. And they are widely used as biological materials in medical devices due to

[1] *State Key Laboratory of Information Photonics and Optical Communications, School of Science, Beijing University of Posts and Telecommunications, Beijing 100876, China.*
[2] *Unit 96911 of PLA, Beijing 100010, China.*
[3] *School of Artificial Intelligence, Beijing University of Posts and Telecommunications, Beijing 100876, China.*
[4] *Ministerial Key Laboratory of ZNDY, Nanjing University of Science &Technology, Nanjing 210094, China.*
[#] *These authors contributed to this work equally.*
**Email:* fefebi@163.com (X. D. Weng); zhaofenghe@bupt.edu.cn (Z. F. He); pxchxc@njust.edu.cn (X. C. Pan); mlei@bupt.edu.cn (M. Lei)

their high biocompatibility, non-toxicity, swelling, and biological bonding properties.[40,41] In addition, as hydrogel itself had hydrophilia and elastic modulus similar to that of skin, it can better fit the skin rather than cause discomfort.[42] While ordinary hydrogels are non-conductive, cannot identify human behavior through changes in electrical signals. To make hydrogels have good electrical conductivity and maintain their original excellent mechanical properties, we can prepare conductive hydrogels by adding conductive nanomaterials, ionic suspended substance groups, and salts in the synthesis process.[43-47] The conductivity is mainly achieved by adding conductive filler to the elastic three-dimensional network of hydrogel to form a conductive path. In principle, the shape change of the conductive hydrogel caused by human behavior will lead to the change of the conductive path inside the hydrogel and the change of the resistance of the hydrogel. However, many reported conductive hydrogels to have to undergo a long preparation process,[6,7] which is complex and is not conducive to the large-scale preparation and application of hydrogels. Thus, it is of great significance to construct an efficient and convenient conductive hydrogel preparation system.

In this paper, conductive polyvinyl alcohol/silver nanoparticles (PVA/AgNPs) hydrogel sensor was prepared by a simple and efficient method of doping silver nanoparticles (AgNPs)[48-50] into the 3D network of polyvinyl alcohol (PVA) hydrogels. Its biocompatibility was guaranteed because of the two materials.[51] The PVA/AgNPs hydrogel sensor had a large draw ratio which was over 500%. The sensor test results showed that it could sensitively receive the electrical signal changes caused by the behavior of the minimum 0.5% shape variable. It also had stretch and release response times of 758 ms and 536 ms. It could still maintain the same resistance change rate as the original after 1000 times of repeated stretching, reflecting its high stability. Several kinds of sensing tests in common human behaviors, such as finger and wrist bending, swallowing, and nodding, suggest that the hydrogel had good performance in practical behavior monitoring. Each PVA/AgNPs hydrogel sensor costs just $1.17. In all, the excellent performance of the PVA/AgNPs hydrogel sensor could be used in flexible wearable devices as a flexible sensor[52] to promote the development of monitoring human behavior.

2. Experimental section

2.1 Materials

Polyvinyl alcohol (1750 ± 50, PVA) was acquired from Sinopharm Chemical Reagent Co., Ltd. Sodium dodecyl sulfate (SDS, AR) was purchased from Aladdin. AgNPs (diameter was 60-150 nm) were purchased from XFNANO, INC. All aqueous solutions used ultrapure water and chemicals were reagent grade without further purification.

2.2 Dispersion of AgNPs

Added AgNPs (0.3 g) to a container containing saturated SDS solution (7 ml) and placed the container in an ultrasonic cleaner. After ultrasonic dispersion for 20 minutes, the AgNPs were uniformly dispersed in the deionized water. A sign of uniform dispersion was that AgNPs do not accumulate at the bottom of the container.

2.3 Preparation of hydrogel sensor

The PVA (1 g) was placed in an ultrasound solution and stirred at 90 °C for 2 h until the PVA was completely dissolved. When the solution was cooled to room temperature, put it into a cold trap at -50 °C to cross-link for 20 min. After thawing at room temperature, the PVA/AgNPs hydrogel sensor was obtained by repeating the freezing cross-linking and thawing process three times.[53,54] The whole preparation process were shown in Fig. S1.

2.4 Characterization

The hydrogels were freeze-dried at -50°C in a vacuum for 7 h. Then, the microstructures were observed by scanning electron microscopy (FE-SEM, LEO-1530, Zeiss, Germany). X-ray diffractometer (XRD, D/max 2500, Rigaku, Japan) with Cu Kα radiation (λ = 1.54178 Å) and X-ray photoelectron spectrometer (Escalab 250Xi) equipped with an Al Kα radiation source (1487.6 eV) were used to characterize the PVA/AgNPs hydrogel sensor.

2.5 Mechanical and electrical properties test

The tensile properties of hydrogels were measured by a universal mechanical tester (Zwicki-Z1.0, ZwickRoell GMbH&Co.KG, Germany). The shapes of hydrogel samples were rectangular (30 × 10 × 3 mm). The real-time resistance of hydrogel sensors upon various deformations was obtained by a combined instrument consisting of a computer-controlled electrochemical workstation (CHI 660E, CH Instrument, China) and a universal mechanical tester (Zwicki-Z1.0, ZwickRoell GMbH&Co.KG, Germany) with a double silver electrode system. The relative resistance change was defined as:[55]

$$\Delta R/R_0\ (\%) = (R - R_0)/R_0 \times 100\% \quad (1)$$

We adopted the method of multiple measurements in the calculation of young's modulus (E). Our experimental value was directly given by the modulus test module in the mechanical testing instrument, and its calculation formula was

$$E = \eta/\varepsilon \quad (2)$$

$$H = F/S \quad (3)$$

$$E = \Delta L/L \quad (4)$$

$$E = FL/S\Delta L \quad (5)$$

where η (kPa) was the force per unit area, F (N) was the force, S (m^2) was the cross-sectional area, ε was the relative deformation under external force, ΔL (m) was the change in length, and L (m) was the initial length. The tangent method was selected for the test. The modulus data given by the system were the tangent slope when the tensile amount was 0%, 25%, 50%, 75%, and 100%. The conductivity calculation formula was:[39]

$$R = U/I = \rho L/S \quad (6)$$

$$\sigma = 1/\rho \quad (7)$$

$$\sigma = IL/US \quad (8)$$

where σ (S/m) was the conductivity, ρ (Ω/m) was resistivity, L (m) was the length of the PVA/AgNPs hydrogel sensor, S (m^2) was the cross-sectional area of the PVA/AgNPs hydrogel sensor, and U (V) and I (A) were the applied voltage and the corresponding current which was available through the electrochemical workstation, respectively. And the formula for calculating GF was[56,57]

$$GF = (\Delta R/R)/\varepsilon \quad (9)$$

3. Results and discussion

3.1 Physical characterization

To verify the doping of AgNPs in the three-dimensional pore structure of the hydrogels, SEM (scanning electron microscopy) images were taken to analyze the microstructure of the hydrogels. The SEM images of the PVA hydrogel sensor (Fig. 1a) showed that the surfaces of hydrogels are smooth. When the silver nanoparticles were doped, they stuck firmly to the surface of the hydrogels' microstructure in the form of AgNPs aggregates about 3 um (Fig. 1b), which was highlighted by red circles. Moreover, AgNPs were doped in the 3D network structure could be explicitly revealed using XRD (Fig. 1c) and X-ray photoelectron spectroscopy (XPS) (Fig. 1d). XRD showed the diffraction peaks of (111), (200), (220), (311) and (222) crystal surfaces of AgNPs. XPS showed the binding energies of Ag 3d electron orbitals, which were consistent with those reported in other literature. The conductive filler was added to the flexible substrate to prepare flexible electronic materials. The conductivity mainly came from the ionic conductivity of the filler.[58] Water was an important part of the conductive network, which could explain why the conductivity of conductive hydrogels became worse after a water loss.

3.2 Mechanical and electrical properties

The conductivity of the conductive hydrogel was 0.02 S/m. As a matter of fact, for conductive hydrogels, the following mechanical properties were required to be flexible sensors, such as strength, deformability, and durability.[59-61] We studied the mechanical and electrical properties of the PVA/AgNPs hydrogel sensor. Photos of several key nodes (0, 100%, 200%, 300%, 400%, and 500%) in the stretching process were shown in Fig. 2a. The PVA/AgNPs hydrogel sensor had excellent stretchability with a maximum form variable of 512%, and breaking strength was 537.7 kPa (Fig. 2b). Such a high tensile resistance made the PVA/AgNPs hydrogel sensor fully adaptable to all kinds of deformation in human behavior monitoring, which was generally difficult to exceed 100%. At the same time, we measured young's modulus of hydrogels with several tensile lengths (Fig. 2c). The value increased with the increase in tensile length. When the stretch length reached 100%, young's modulus was 167.6 kPa. Then, we measured the water loss rate of the PVA/AgNPs hydrogel sensor without stretching and at 150% stretch length (Fig. 2d). The results showed that the water loss rate in the tensile state was higher. At 150% tensile length for 80 min, the mass of hydrogels was still 60% of the original.

For sensors, one of the most important properties was sensitivity, also known as sensing limit.[35,62] Sensitivity determined the suitability of the sensor. The PVA/AgNPs hydrogel sensor had high sensitivity and could detect at least 0.5% deformation, corresponding to a 0.5% resistance change rate (Fig. 2e). Perhaps the sensitivity could be higher, but its measurement was limited by the precision of mechanical testing instruments. Sensitivity was also one of the performance indicators of the reaction sensor. The resistivity change rate-strain curve[56] (Fig. S2a) and resistivity change rate-stress curve (Fig. S2b) were given, and the gauge factor (GF) value and sensitivity were calculated. GF value was 0.75, the sensitivity was divided into two parts, 0.017 kPa^{-1} at 0-22 kPa, and 0.008 kPa^{-1} at 22-115 kPa. The responsiveness of the sensor was reflected by its response time under tensile and relaxation mutation states. The internal structure of the sensor would change dramatically when it was stretched, such as

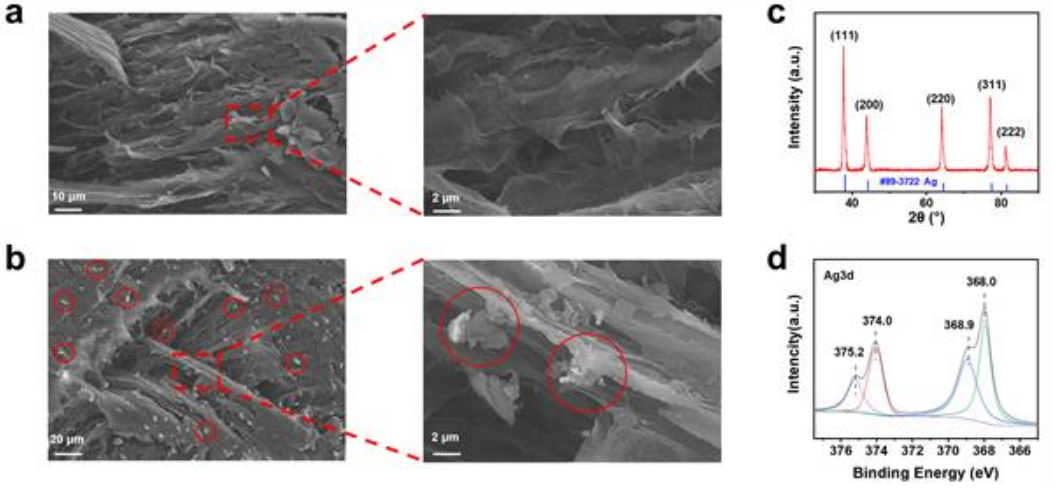

Fig. 1 (a) SEM image of the PVA hydrogel sensor. (b) SEM image of the PVA/AgNPs hydrogel sensor. (c) XRD pattern of the PVA/AgNPs hydrogel sensor. (d) XPS peak-differentiation-imitating of Ag 3d.

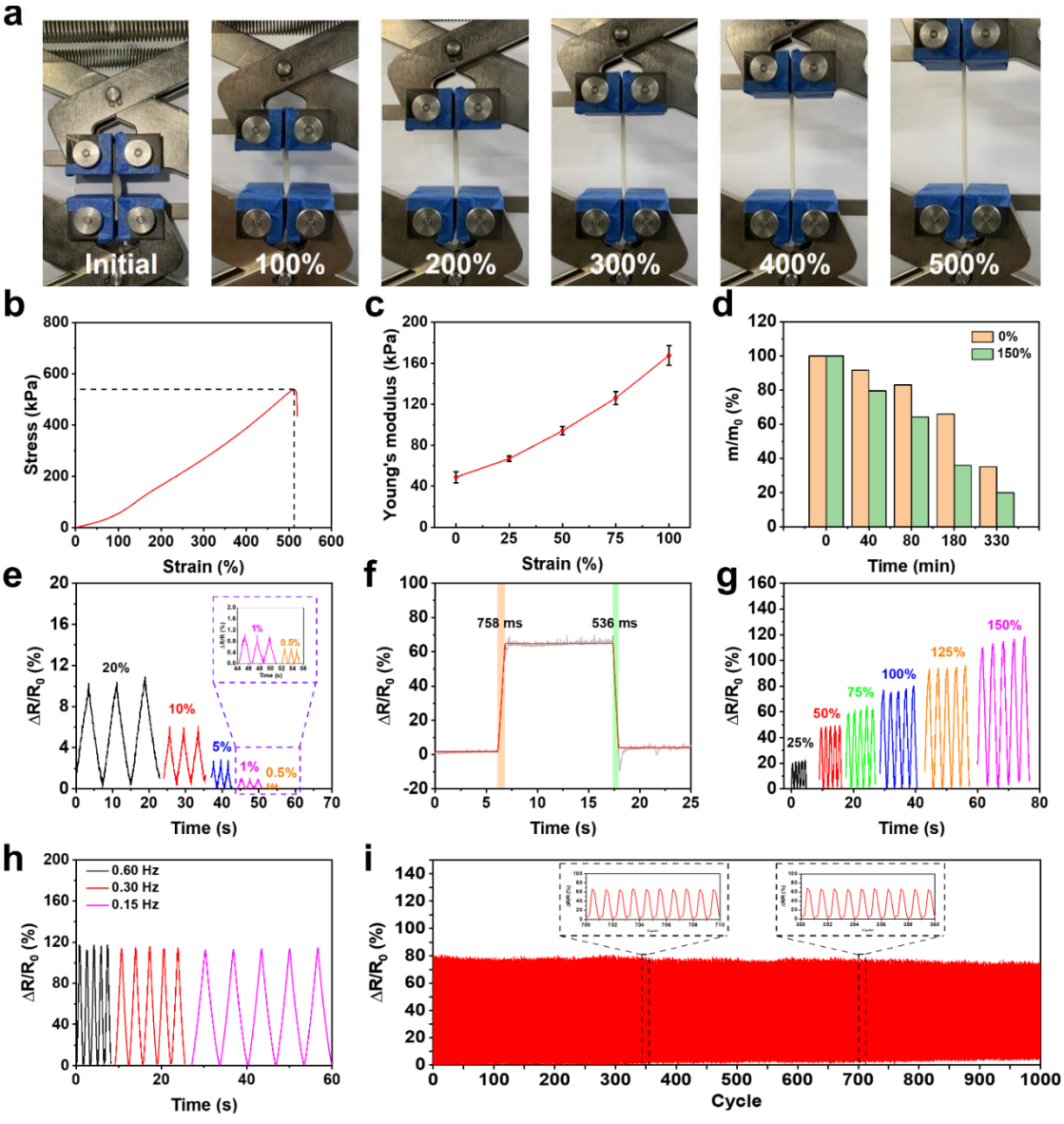

Fig. 2 Mechanical and electrical properties of the PVA/AgNPs hydrogel sensor under stretching. (a) Photos at the different tensile lengths (0, 100%, 200%, 300%, 400%, and 500%). (b) Relationship between tensile length and stress (c) Young's modulus at different lengths. (d) Water loss test. (e) The resistance change rate ($\Delta R/R0$) under several small shape variables. (f) The response time of the sensor during 100% loading and unloading under stretching at a speed of 30 mm/s. (g) The $\Delta R/R0$ under various tensile strains (0, 25%, 50%, 75%, 100%, 125%, and 150%). (h) The $\Delta R/R0$ with different stretching frequencies (0.60Hz, 0.30Hz, and 0.15Hz) at the strain of 150%. (i) The $\Delta R/R0$ from 0 to 100% tensile length for 1000 cycles with a speed of 20 mm/s.

local carrier concentration and conduction distance. These changes made it impossible for the sensor to respond to the measured changes immediately and took some time to respond. And the lag time was the response time. Our hydrogel tensile response time was 758 ms, while the stress release response time was 536 ms, reflecting the quick response capability of the hydrogel sensor (Fig. 2f). In addition, the PVA/AgNPs hydrogel sensor showed excellent stability in both tensile modes. In the first case, we selected different tensile lengths (0, 25%, 50%, 75%, 100%, 125%, and 150%) at the same stretching frequency which was 0.60Hz (Fig. 2g). The sensor exhibited an almost linear variation and remains stable at these tensile lengths. The second was the same amount of stretching with different stretching frequencies (0.60Hz, 0.30Hz, and 0.15Hz), and the tensile length was 150% (Fig. 2h). Although the sensor had different stress recovery at different speeds, the resistance change rate remained stable at around 120%. It was very important for detecting complex motion quickly and in time. Then, we continued the PVA/AgNPs hydrogel sensor at 100% tensile length, 1000 cycles of the cyclic tensile test (Fig. 2h). Although it was prone to structural changes caused by water loss in the process of drawing, so far as the resistance changes greatly, it still showed excellent repeatable tensile properties in the test. This long-cycle test proved that hydrogels could be applied to more practical situations. The PVA/AgNPs hydrogel sensor was a piezoresistive sensor based on the piezoresistive effect. It responded to strain mainly by changing the resistance when being stretched. The more

severe the strain was, the more the resistance changed. The conductive mechanism of the doped sensor as described above utilizes the ionic conductive mode of the conductive filler. Moreover, the piezoresistive effect of composites was generally considered to be determined by the relative change of AgNPs content caused by the great difference of elastic modulus between AgNPs and PVA hydrogel matrix.[63] However, the negative effect of the increase of the length on the relative content of AgNPs was far greater than the positive effect of the decrease of the cross-sectional area on the relative content of AgNPs. Therefore, in general, the relative content of AgNPs decreased and the composite resistivity increased, leading to an increase in the sensor resistance.

We summarized and compared the mechanical and electrical properties of the AgNPs hydrogel sensor with some published hydrogels, and relevant data were presented in Table S1.[56,64-70] The sensing type of all sensors was piezoresistive. Most of them took organic conductive materials or conductive carbon materials as fillers and used the connections between fibrous structures to construct conductive paths. Most of the conductive types were electronic conductive. The AgNPs hydrogel sensor prepared in this work mainly used the ionic conductive form of metal filler in the 3D structure of PVA. The conductive form would directly affect the conductivity of the hydrogel, which was also the reason for the low conductivity of the AgNPs hydrogel sensor. At the same time, it also affected GF value to a certain extent. But the sensitivity of the AgNPs hydrogel sensor was comparable to other sensors in the same range, and could even be applied to a larger pressure range. In addition, the tensile properties of the AgNPs hydrogel sensor were also good, and the 500% strain was sufficient to meet almost all human behavior monitoring. The low modulus also made it relatively easy for the sensor to respond to stress. It was worth noting that the advantages of the AgNPs hydrogel sensor also lay in the simplicity of preparation and high reusability. The raw material could be used without reprocessing, and such a preparation method was suitable for most metal nanoparticles. And the high reuse performance of 1000 times 100% strain stretching was much higher than other sensors.

3.3 Human behavior monitoring applications

Due to the excellent performance of the PVA/AgNPs hydrogel sensor in pressure sensing, to verify the feasibility of using it as a wearable strain sensor to monitor a variety of human behaviors, we recorded the electrical signals of four behaviors to verify. First, the PVA/AgNPs hydrogel sensor was fixed at the second joint of the index finger and real-time electrical signals of different degrees of bending of the index finger were recorded (Fig. 3a). Bending degrees were about 0, 30°, and 60°, and 90°. The illustration was the actual bending. The results showed that the differences in electrical signals with different degrees of bending were obvious. Then we put the PVA/AgNPs hydrogel sensor on the wrist and the bending of

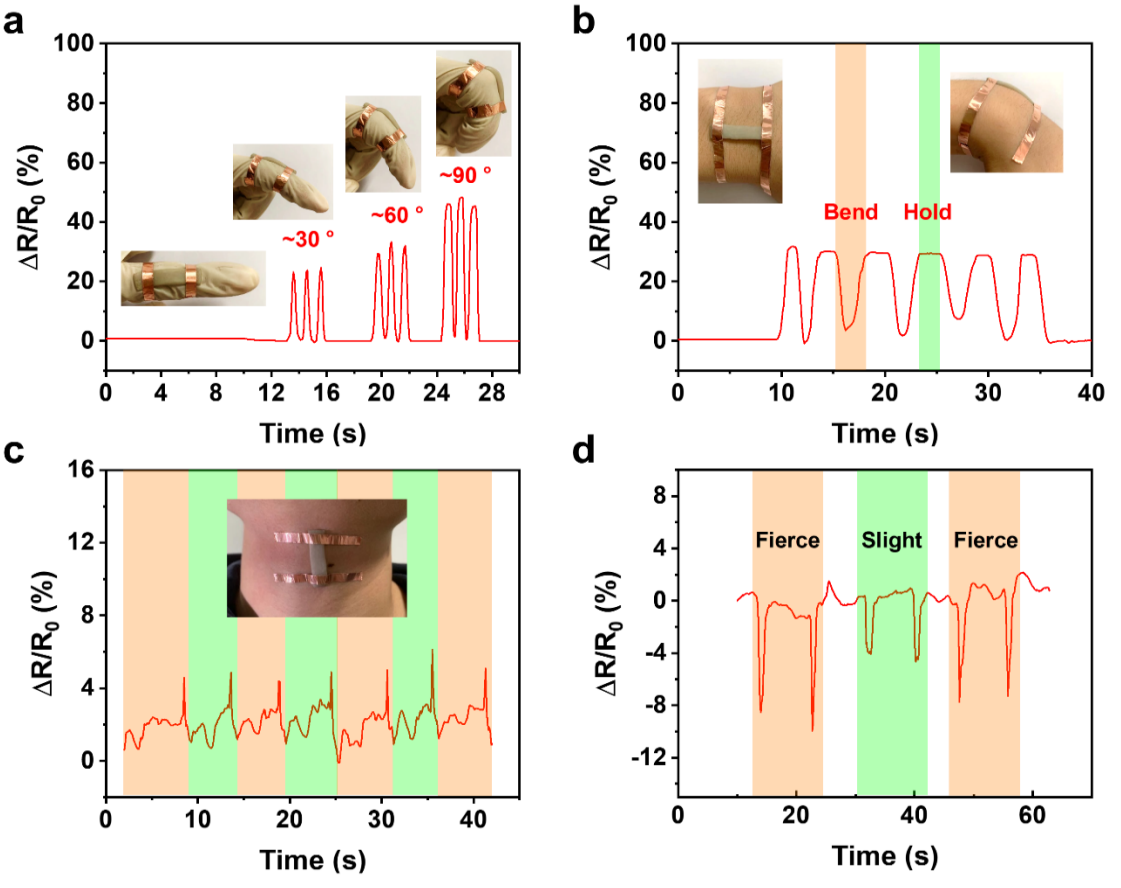

Fig. 3 Application scenario of the PVA/AgNPs hydrogel sensor. (a) The $\Delta R/R_0$ for finger bending at different angles. (b) The $\Delta R/R_0$ for wrist bending. (c) The $\Delta R/R_0$ for making some swallowing. (d) The $\Delta R/R_0$ for the nod.

the wrist also caused the electrical signals to change without a doubt (Fig. 3b). When the wrist maintained a posture for some time, it could also be reflected in the electrical signal. Furthermore, some minor behaviors could also cause significant changes in hydrogel sensor electrical signals, such as swallowing (Fig. 3c). We could clearly distinguish the electrical signals of each swallowing action, and the electrical signals of this action also had a high consistency. In particular, because the PVA/AgNPs hydrogel sensor was made into long strips, the compression process was relatively difficult to achieve. However, in the monitoring process of nodding behavior, we found that the resistance change rate was negative and the electrical signals were also easily distinguished (Fig. 3d). A negative value of the resistance represented a decrease in the length of the hydrogel, which corresponded to actual muscle contraction during nodding. In this process, the PVA/AgNPs hydrogel sensor was glued to the neck where meets the chin.

4. Conclusions

In summary, we prepared conductive the PVA/AgNPs hydrogel sensor by a simple and efficient method of doping AgNPs into the PVA hydrogels network. The PVA/AgNPs hydrogel sensor had a large draw ratio of over 500%. The hydrogels sensitively could receive the electrical signal changes caused by the behavior of the minimum 0.5% shape variable. Stretch and release response times were 758 ms and 536 ms, respectively. These properties suggested that hydrogels could achieve rapid response to small behavioral changes. Besides, the sensor had excellent repeatability and stability. Its resistance change rate remained stable after 1000 cycles of stretching. The PVA/AgNPs hydrogel sensor showed good performance in practical behavior monitoring. The sensor could respond obviously to signal changes caused by large movements such as finger and wrist bending, and small movements like swallowing. The mechanical and sensing properties supported it to be an excellent pressure resistance sensor. Its low price will make it the potential for large-scale production and commercial application.

Acknowledgments

This study was supported financially by the Fundamental Research Funds for the Central Universities (2021XD-A04-1), the National Natural Science Foundation of China (Nos. 61874014 and 61874013), and the Fund of State Key Laboratory of Information Photonics and Optical Communications (Beijing University of Posts and Telecommunications, P.R. China).

Conflict of interest

There are no conflicts to declare.

Supporting information

Applicable.

References

[1] B. A. Kuzubasoglua, S. K. Bahadir, *Sensors and Actuators A: Physical*, 2020, **315**, 112282, doi: 10.1016/j.sna.2020.112282.
[2] H. Jiang, L. Zheng, Z. Liu, X. Wang, *InfoMat*, 2020, **2**, 1077-1094, doi: 10.1002/inf2.12072.
[3] J. Yu, X. Yang, Q. Sun, *Advanced Intelligent Systems*, 2020, **2**, 1900175, doi: 10.1002/aisy.201900175.
[4] Y. Li, J. Guo, M. Li, Y. Tang, V. Murugadoss, I. Seok, J. Yu, L. Sun, C. Sun, Y. Luo, *ES Food & Agroforestry*, 2021, **4**, 9-27, doi: 10.30919/esfaf466.
[5] N. Wen, L. Zhang, D. Jiang, Z. Wu, B. Li, C. Sun, Z. Guo, *Journal of Materials Chemistry A*, 2020, **8**, 25499-25527, doi: 10.1039/d0ta09556g.
[6] Y. Gao, J. Peng, M. Zhou, Y. Yang, X. Wang, J. Wang, Y. Cao, W. Wang, D. Wu, *Journal of Materials Chemistry B*, 2020, **8**, 11010-11020, doi: 10.1039/d0tb02250k.
[7] C. Wang, K. Hu, C. Zhao, Y. Zou, Y. Liu, X. Qu, D. Jiang, Z. Li, M. R. Zhang, Z. Li, *Small*, 2020, **16**, 1904758, doi: 10.1002/smll.201904758.
[8] Y. Xi, J. Hua, Y. Shi, *Nano Energy*, 2020, **69**, 104390, doi: 10.1016/j.nanoen.2019.104390.
[9] D. Rohilla, S. Chaudhary, A. Umar, *Engineered Science*, 2021, **16**, 47-70, doi: 10.30919/es8d552.
[10] S. Lin, X. Bai, H. Wang, H. Wang, J. Song, K. Huang, C. Wang, N. Wang, B. Li, M. Lei, H. Wu, *Advanced Materials*, 2017, **29**, 1703238, doi: 10.1002/adma.201703238.
[11] H. Huang, L. Han, Y. Wang, Z. Yang, F. Zhu, M. Xu, *Engineered Science*, 2020, **9**, 60-67, doi: 10.30919/es8d812.
[12] S. Lin, H. Wang, F. Wu, Q. Wang, X. Bai, D. Zu, J. Song, D. Wang, Z. Liu, Z. Li, N. Tao, K. Huang, M. Lei, B. Li, H. Wu, *Npj Flexible Electronics*, 2019, **3**, 6, doi: 10.1038/s41528-019-0050-8.
[13] J. Liu, S. Lin, K. Huang, C. Jia, Q. Wang, Z. Li, J. Song, Z. Liu, H. Wang, M. Lei, H. Wu, *Npj Flexible Electronics*, 2020, **4**, 10, doi: 10.1038/s41528-020-0074-0.
[14] X. Chang, L. Chen, J. Chen, Y. Zhu, Z. Guo, *Advanced Composites and Hybrid Materials*, 2021, **4**, 435-450, doi: 10.1007/s42114-021-00292-3.
[15] Y. Huang, Y. Luo, H. Liu, X. Lu, J. Zhao, Y. Lei, *Engineered Science*, 2021, **14**, 59-68, doi: 10.30919/es8d1161.
[16] Y. Guo, M. Zhong, Z. Fang, P. Wan, G. Yu, *Nano Letters*, 2019, **19**, 1143-1150, doi: 10.1021/acs.nanolett.8b04514.
[17] S. Lim, D. Son, J. Kim, Y. B. Lee, J. K. Song, S. Choi, D. J. Lee, J. H. Kim, M. Lee, T. Hyeon, D. H. Kim, *Advanced Functional Materials*, 2015, **25**, 375-383, doi: 10.1002/adfm.201402987.
[18] E. Roh, B. U. Hwang, D. Kim, B. Y. Kim, N. E. Lee, *ACS Nano*, 2015, **9**, 6252-6261, doi: 10.1021/acsnano.5b01613.
[19] E. J. Markvicka, M. D. Bartlett, X. Huang, C. Majidi, *Nature Materials*, 2018, **17**, 618-624, doi: 10.1038/s41563-018-0084-7.
[20] N. Lu, D. H. Kim, *Soft Robotics*, 2014, **1**, 53-62, doi: 10.1089/soro.2013.0005.
[21] Z. Liu, Y. Wang, Y. Ren, G. Jin, C. Zhang, W. Chen, F. Yan, *Materials Horizons*, 2020, **7**, 919-927, doi: 10.1039/c9mh01688k.
[22] J. Wei, X. Chu, X. Y. Sun, K. Xu, H. X. Deng, J. Chen, Z.

Wei, M. Lei, *InfoMat*, 2019, **1**, 338-358, doi: 10.1002/inf2.12028.
[23] C. Mu, Y. Song, W. Huang, A. Ran, R. Sun, W. Xie, H. Zhang, *Advanced Functional Materials*, 2018, **28**, 1707503, doi: 10.1002/adfm.201707503.
[24] M. S. Suen, Y. C. Lin, R. Chen, *Sensors and Actuators A: Physical*, 2018, **269**, 574-584, doi: 10.1016/j.sna.2017.11.053.
[25] M. Chen, X. Hu, K. Li, J. Sun, Z. Liu, B. An, X. Zhou, Z. Liu, *Carbon*, 2020, **164**, 111-120, doi: 10.1016/j.carbon.2020.03.042.
[26] J. Chen, Y. Zhu, Z. Guo, A. G. Nasibulin, *Engineered Science*, 2020, **12**, 13-22, doi: 10.30919/es8d1129.
[27] J. Chen, Y. Zhu, X. Chang, D. Pan, G. Song, Z. Guo, N. Naik, *Advanced Functional Materials*, 2021, **31**, 2104686, doi: 10.1002/adfm.202104686.
[28] Y. Pang, H. Tian, L. Tao, Y. Li, X. Wang, N. Deng, Y. Yang, T. L. Ren, *ACS Applied Materials & Interfaces*, 2016, **8**, 26458-26462, doi: 10.1021/acsami.6b08172.
[29] D. Zhang, B. Chi, B. Li, Z. Gao, Y. Du, J. Guo, J. Wei, *Synthetic Metals*, 2016, **217**, 79-86, doi: 10.1016/j.synthmet.2016.03.014.
[30] M. Wang, K. Zhang, X. X. Dai, Y. Li, J. Guo, H. Liu, G. H. Li, Y. J. Tan, J. B. Zeng, Z. Guo, *Nanoscale*, 2017, **9**, 11017-11026, doi: 10.1039/c7nr02322g.
[31] Z. Sun, S. Fang, Y. H. Hu, *Chemical Reviews*, 2020, **120**, 10336-10453, doi: 10.1021/acs.chemrev.0c00083.
[32] B. Cheng, Y. Li, H. Li, H. Li, S. Yang, P. Li, Y. Shang, *Composites Science and Technology*, 2021, **213**, 108948, doi: 10.1016/j.compscitech.2021.108948.
[33] S. Gong, W. Schwalb, Y. Wang, Y. Chen, Y. Tang, J. Si, B. Shirinzadeh, W. Cheng, *Nature Communications*, 2014, **5**, 3132, doi: 10.1038/ncomms4132.
[34] B. Hu, W. Chen, J. Zhou, *Sensors and Actuators B: Chemical*, 2013, **176**, 522-533, doi: 10.1016/j.snb.2012.09.036.
[35] C. Pang, G. Y. Lee, T. I. Kim, S. M. Kim, H. N. Kim, S. H. Ahn, K. Y. Suh, *Nature Materials*, 2012, **11**, 795-801, doi: 10.1038/nmat3380.
[36] V. R. Feig, H. Tran, M. Lee, Z. Bao, *Nature Communications*, 2018, **9**, 2740, doi: 10.1038/s41467-018-05222-4.
[37] Q. Ding, X. Xu, Y. Yue, C. Mei, C. Huang, S. Jiang, Q. Wu, J. Han, *ACS Applied Materials & Interfaces*, 2018, **10**, 27987-28002, doi: 10.1021/acsami.8b09656.
[38] Y. Zhou, C. Wan, Y. Yang, H. Yang, S. Wang, Z. Dai, K. Ji, H. Jiang, X. Chen, Y. Long, *Advanced Functional Materials*, 2019, **29**, 1806220, doi: 10.1002/adfm.201806220.
[39] S. Lin, J. Liu, W. Li, D. Wang, Y. Huang, C. Jia, Z. Li, M. Murtaza, H. Wang, J. Song, Z. Liu, K. Huang, D. Zu, M. Lei, B. Hong, H. Wu, *Nano Letters*, 2019, **19**, 6853-6861, doi: 10.1021/acs.nanolett.9b02019.
[40] M. I. Baker, S. P. Walsh, Z. Schwartz, B. D. Boyan, *Journal of Biomedical Materials Research Part B: Applied Biomaterials*, 2012, **100**, 1451-1457, doi: 10.1002/jbm.b.32694.
[41] S. R. Prasad, S. B. Teli, J. Ghosh, N. R. Prasad, V. S. Shaikh, G. M. Nazeruddin, A. G. Al-Sehemi, I. Patel, Y. I. Shaikh, *Engineered Science*, 2021, **16**, 90-128, doi: 10.30919/es8d479.
[42] F. Gao, Y. Y. Zhang, Y. M. Li, B. Xu, Z. Q. Cao, W. G. Liu, *ACS Applied Materials and Interfaces*, 2016, **8**, 8956-8966, doi: 10.1021/acsami.6b00912.
[43] Z. Deng, Y. Guo, X. Zhao, P. X. Ma, B. Guo, *Chemistry of Materials*, 2018, **30**, 1729-1742, doi: 10.1021/acs.chemmater.8b00008.
[44] G. Ge, Y. Zhang, J. Shao, W. Wang, W. Si, W. Huang, X. Dong, *Advanced Functional Materials*, 2018, **28**, 1802576, doi: 10.1002/adfm.201802576.
[45] T. Wang, Wusigale, D. Kuttappan, M. A. Amalaradjou, Y. Luo, Y. Luo, *Advanced Composites and Hybrid Materials*, 2021, **4**, 696-706, doi: 10.1007/s42114-021-00305-1.
[46] H. Wei, A. Li, D. Kong, Z. Li, D. Cui, T. Li, B. Dong, Z. Guo, *Advanced Composites and Hybrid Materials*, 2021, **4**, 86-95, doi: 10.1007/s42114-020-00201-0.
[47] W. Zhao, L. Chen, S. Hu, Z. Shi, X. Gao, V. V. Silberschmidt, *Advanced Composites and Hybrid Materials*, 2020, **3**, 315-324, doi: 10.1007/s42114-020-00161-5.
[48] R. Quhe, L. Xu, S. Liu, C. Yang, Y. Wang, H. Li, J. Yang, Q. Li, B. Shi, Y. Li, Y. Pan, X. Sun, J. Li, M. Weng, H. Zhang, Y. Guo, L. Xu, H. Tang, J. Dong, J. Yang, Z. Zhang, M. Lei, F. Pan, J. Lu, *Physics Reports*, 2021, **938**, 1-72, doi: 10.1016/j.physrep.2021.07.006.
[49] W. J. Liu, M. L. Liu, S. Lin, J. C. Liu, M. Lei, H. Wu, C. Q. Dai, Z. Y. Wei, *Optics Express*, 2019, **27**, 16440, doi: 10.1364/oe.27.016440.
[50] S. Lin, H. Wang, X. Zhang, D. Wang, D. Zu, J. Song, Z. Liu, Y. Huang, K. Huang, N. Tao, Z. Li, X. Bai, B. Li, M. Lei, Z. Yu, H. Wu, *Nano Energy*, 2019, **62**, 111-116, doi: 10.1016/j.nanoen.2019.04.071.
[51] L. Y. Wei, J. R. Lu, H. Z. Xu, A. Patel, Z. S. Chen, G. F. Chen, *Drug Discovery Today*, 2015, **20**, 595-601, doi: 10.1016/j.drudis.2014.11.014.
[52] K. Xu, Y. Lu, K. Takei, *Advanced Materials Technologies*, 2019, **4**, 1800628, doi: 10.1002/admt.201800628.
[53] K. Huang, L. Junchen, S. Lin, Y. Wu, E. Chen, Z. He, M. Lei, *Advanced Composites and Hybrid Materials*, 2021, **5**, 1-9, doi: 10.1007/s42114-021-00322-0.
[54] S. Lin, J. Liu, Q. Wang, D. Zu, H. Wang, F. Wu, X. Bai, J. Song, Z. Liu, Z. Li, K. Huang, B. Li, M. Lei, H. Wu, *Advanced Materials Technologies*, 2020, **5**, 1900761, doi: 10.1002/admt.201900761.
[55] Y. Wu, J. Liu, S. Lin, K. Huang, E. Chen, K. Huang, M. Lei, *Engineered Science*, 2022, **18**, 105-112, doi: 10.30919/es8d626.
[56] J. Zhang, L. Chen, B. Shen, Y. Wang, P. Peng, F. Tang, J. Feng, *Materials Science and Engineering: C*, 2020, **117**, 111298, doi: 10.1016/j.msec.2020.111298.
[57] K. Huang, Y. Wu, J. Liu, G. Chang, X. Pan, X. Weng, Y. Wang, M. Lei, *Engineered Science*, 2022, **17**, 319–327, doi: 10.30919/es8d625.
[58] F. Fu, J. Wang, H. Zeng, J. Yu, *ACS Materials Letters*, 2020, **2**, 1287-1301, doi: 10.1021/acsmaterialslett.0c00309.
[59] M. Lou, I. Abdalla, M. Zhu, J. Yu, Z. Li, B. Ding, *ACS Applied Materials & Interfaces*, 2020, **12**, 1597-1605, doi: 10.1021/acsami.9b19238.
[60] Y. J. Tan, H. Godaba, G. Chen, S. T. M. Tan, G. Wan, G. Li,

P. M. Lee, Y. Cai, S. Li, R. F. Shepherd, J. S. Ho, B. C. K. Tee, *Nature Materials*, 2020, **19**, 182-188, doi: 10.1038/s41563-019-0548-4.
[61] L. Wang, S. Xie, Z. Wang, F. Liu, Y. Yang, C. Tang, X. Wu, P. Liu, Y. Li, H. Saiyin, S. Zheng, X. Sun, F. Xu, H. Yu, H. Peng, *Nature Biomedical Engineering*, 2019, **4**, 159-171, doi: 10.1038/s41551-019-0462-8.
[62] L. Viry, A. Levi, M. Totaro, A. Mondini, V. Mattoli, B. Mazzolai, L. Beccai, *Advanced Materials*, 2014, **26**, 2659-2664, doi: 10.1002/adma.201305064.
[63] Z. Wang, X. Ye, *Nanotechnology*, 2014, **25**, 285502, doi: 10.1088/0957-4484/25/28/285502.
[64] Y. Zhang, E. Ren, A. Li, C. Cui, R. Guo, H. Tang, H. Xiao, M. Zhou, W. Qin, X. Wang, L. Liu, *Journal of Materials Chemistry B*, 2021, **9**, 719-730, doi: 10.1039/d0tb01926g.
[65] Y. Lu, J. Han, Q. Ding, Y. Yue, C. Xia, S. Ge, Q. van le, X. Dou, C. Sonne, S. S. Lam, *Cellulose*, 2021, **28**, 1469-1488, doi: 10.1007/s10570-020-03606-8.
[66] Y. Lu, Y. Yue, Q. Ding, C. Mei, X. Xu, Q. Wu, H. Xiao, J. Han, *ACS Applied Materials & Interfaces*, 2021, **13**, 50281-50297, doi: 10.1021/acsami.1c16828.
[67] L. Kong, Z. Gao, X. Li, G. Gao, *Journal of Materials Chemistry B*, 2021, **9**, 1082-1088, doi: 10.1039/d0tb02460k.
[68] Y. Jiao, Y. Lu, K. Lu, Y. Yue, X. Xu, H. Xiao, J. Li, J. Han, *Journal of Colloid and Interface Science*, 2021, **597**, 171-181, doi: 10.1016/j.jcis.2021.04.001.
[69] H. Zheng, N. Lin, Y. He, B. Zuo, *ACS Applied Materials & Interfaces*, 2021, **13**, 40013-40031, doi: 10.1021/acsami.1c08395.
[70] C. Zheng, K. Lu, Y. Lu, S. Zhu, Y. Yue, X. Xu, C. Mei, H. Xiao, Q. Wu, J. Han, *Carbohydrate Polymers*, 2020, **250**, 116905, doi: 10.1016/j.carbpol.2020.116905.

Author information

Yufeng Wu *received his B.D. at Northeast Normal University in 2019. Now, he is pursuing his Ph.D. in Beijing University of Posts and Telecommunications. His research interest is the fabrication, assembly and application of flexible sensors.*

Enfu Chen *received his B.D. at Beijing University of Posts and Telecommunications in 2019. Now, he is pursuing his M.D. at Beijing University of Posts and Telecommunication s. His research interest is hydrogel sensor.*

Ming Lei *received his M.D. at State Key Laboratory of Materials Composites and Advanced Technology, Wuhan University of Technology in 2004. Then, he received his Ph.D. from the Laboratory of Nanophysics and Devices, Institute of Physics, Chinese Academy of Sciences in 2007. He worked as a postdoctoral fellow at The Hong Kong University of Science and Technology (2007-2008) and the Chinese University of Hong Kong (2009-2010). He is now a professor and doctoral supervisor of the School of Science, Beijing University of Posts and Telecommunications. He has long been engaged in the preparation of low dimensional nano materials, photoelectric properties and device applications.*